

Noise Enhancement of Period Doubling in Strongly Modulated Semiconductor Lasers

This content has been downloaded from IOPscience. Please scroll down to see the full text.

1992 Jpn. J. Appl. Phys. 31 L846

(<http://iopscience.iop.org/1347-4065/31/7A/L846>)

View [the table of contents for this issue](#), or go to the [journal homepage](#) for more

Download details:

IP Address: 140.113.38.11

This content was downloaded on 28/04/2014 at 17:55

Please note that [terms and conditions apply](#).

Noise Enhancement of Period Doubling in Strongly Modulated Semiconductor Lasers

Yao Huang KAO, Hung Tser LIN and Ching Sheu WANG¹

*Department of Communication Engineering and Center of Telecommunication Research,
 National Chiao-Tung University, 1001 Ta Hsueh Road, Hsin-Chu, Taiwan, 30050, R.O.C.*

¹*Institute of Electro-Optical Engineering, National Chiao-Tung University,
 1001 Ta Hsueh Road, Hsin-Chu, Taiwan, 30050, R.O.C.*

(Received December 16, 1991; accepted for publication May 16, 1992)

In this paper the phenomena of period doubling and bistability of multiple spiking states in deeply modulated laser diodes are investigated. The situations of in which the period doubling in the parameter space occurs are indicated. The influence of noise on the period doubling is examined by employing the single-mode rate equations with Langevin noise.

KEYWORDS: period doubling, bistability, Langevin noise, semiconductor laser

§1. Introduction

Recently, strong current modulation in semiconductor laser diodes has received much attention, especially in microwave analog fiber-optic transmission.¹⁻⁷⁾ Under such circumstances, modulated laser diodes exhibit a number of nonlinear phenomena, such as harmonic distortion, bistability, and period doubling (PD) route to chaos. In the semiclassical approach, the nonlinear rate equations governing the interrelationship between carrier density and photon density have been successfully applied to predict the relaxation oscillation and bistability.^{3,5)} Also, the influences of the nonlinear gain suppression factor, spontaneous emission factor, and Auger recombination factor on the period doubling phenomenon have been examined numerically.^{3,4,6)} To date, despite great efforts, the important role of noise on the dynamics of the routes to chaos has not yet been explored in detail. In fact, the output of a cw diode laser exhibits large amplitude fluctuation with a frequency centered at the relaxation oscillation resonance.⁸⁾ These fluctuations arise from the quantum nature of spontaneous emission and cannot be eliminated in real diode lasers. In this letter we examine the phenomenon of period doubling under deep modulation and pay special attention to the noise effect on the first onset of period doubling.

§2. Stochastic Rate Equations

With consideration of nonlinear gain suppression and the Langevin noise terms, the stochastic single-mode rate equations for the photon density S and carrier density n can be written as⁵⁾

$$\frac{dn}{dt} = \frac{I(t)}{eV} - \frac{n}{\tau_e} - A(1 - \varepsilon_{nl}S)(n - n_0)S + F_n(t)/V, \quad (1)$$

$$\frac{dS}{dt} = \Gamma A(1 - \varepsilon_{nl}S)(n - n_0)S - \frac{S}{\tau_p} + \frac{\Gamma\beta n}{\tau_e} + F_s(t)/V, \quad (2)$$

where e is the electron charge, V is the active volume, τ_e and τ_p are the electron and photon lifetimes, respectively, A is the gain constant, n_0 is the carrier density for

transparency, Γ is the confinement factor, β is the spontaneous emission factor, and ε_{nl} is the nonlinear gain suppression factor. For the sake of comparison, typical values of parameters are chosen: $V = 2.5 \times 10^{-16} \text{ m}^3$, $\tau_e = 3 \text{ ns}$, $\tau_p = 6 \text{ ps}$, $A = 2.5 \times 10^{-7}$, $n_0 = 1.5 \times 10^{18} \text{ cm}^{-3}$, $\Gamma = 1$, and $\beta = 5 \times 10^{-5}$, as in refs. 3 and 5. The driving current containing dc and ac terms can be expressed as $I(t) = I_{dc} + I_{ac} \sin(2\pi ft)$. F_s and F_n are Langevin noise sources with mean values of zero that arise from spontaneous emission and from the discrete nature of the carrier generation and recombination, respectively. These noise processes are assumed to be Gaussian random variables. Under the Markovian assumptions, the autocorrelation and cross-correlation functions of F_s and F_n are proportional to the Dirac delta functions and can be expressed as⁹⁾

$$\langle F_n(t)F_n(t') \rangle = V_n^2 \delta(t - t') \quad (3)$$

$$\langle F_s(t)F_s(t') \rangle = V_s^2 \delta(t - t') \quad (4)$$

$$\langle F_n(t)F_s(t') \rangle = \gamma_0 V_n V_s \delta(t - t'), \quad (5)$$

where V_n and V_s are the variances of F_n and F_s , respectively, and γ_0 is the correlation coefficient and is equal to one for the single-mode case. According to Marcuse,⁹⁾ the variances can be expressed as follows:

$$V_n^2 = I/e + nV/\tau_e + A(1 + \varepsilon_{nl}S)(n + n_0)SV, \quad (6)$$

$$V_s^2 = SV/\tau_p + \Gamma A(1 + \varepsilon_{nl}S)(n + n_0)SV + \Gamma\beta nV/\tau_e, \quad (7)$$

$$V_n V_s = -\{\Gamma\beta nV/\tau_e + \Gamma A(1 + \varepsilon_{nl}S)(n + n_0)SV\}. \quad (8)$$

The expressions for the variances closely resemble the right-hand sides of the rate eqs. (1) and (2), except that all terms have positive signs. This is because each term of the rate equations acts as a source of shot noise.

Here, the responses of eqs. (1) and (2) are calculated by employing the fourth-order Runge-Kutta algorithm. The stochastic functions F_s and F_n in any particular time interval Δt can be treated as $F_s = V_s X_s / \Delta t^{1/2}$ and $F_n = V_n X_n / \Delta t^{1/2}$ with X_s and X_n denoting a Gaussian random variable of zero mean and unit variance. Furthermore, for numerical purposes, the photon density and carrier density in eqs. (1) and (2) are normalized by defining

$P=S/S_0$ and $N=n/n_{th}$ with constant $S_0=\Gamma(\tau_p/\tau_e)n_{th}$ and the threshold carrier density $n_{th}=n_0+(\Gamma A\tau_p)^{-1}$; then the rate equations become

$$\frac{dN}{dt}=\frac{1}{\tau_e}\left(\frac{I(t)}{I_{th}}-N-\frac{N-\delta}{1-\delta}(1-\varepsilon P)P\right)+F'_n, \quad (9)$$

$$\frac{dP}{dt}=\frac{1}{\tau_p}\left(\frac{N-\delta}{1-\delta}(1-\varepsilon P)P-P+\beta N\right)+F'_s, \quad (10)$$

where

$$F'_n=\left[\frac{\left(\frac{I(t)}{I_{th}}+N+\frac{N+\delta}{1-\delta}(1+\varepsilon P)P\right)^{1/2}}{\tau_e\Delta tVn_{th}}\right]X_n,$$

$$F'_s=\left[\frac{\left(\frac{N+\delta}{1-\delta}(1+\varepsilon P)P+P+\beta N\right)^{1/2}}{\tau_p\Delta tVS_0}\right]X_s,$$

the constants $\delta=n_0/n_{th}(=0.692)$, the threshold current $I_{th}=eVn_{th}/\tau_e$, and $\varepsilon=\varepsilon_{nl}S_0$. It is expected that ε is somewhat lower than 10^{-4} for GaAs lasers, and larger than 10^{-2} for InGaAsP lasers.⁵⁾ The normalized dc bias and ac-modulated currents are defined as $I_b=I_{dc}/I_{th}$ and $m=I_{ac}/I_{th}$. The latter is also denoted as the modulation index. During the computation the time interval Δt is chosen as $\Delta t=T/128$, where T is the period of the driving current. This ascertains that the noise spectrum is approximately white within twice the driving frequency, as demonstrated in the simulation. The calculation has been extended to 1200 cycles. The power spectra are then calculated using a fast Fourier transform with 4096 time points. To improve the accuracy, the Fourier spectra shown in Fig. 4 are determined by averaging over 32 spectral components, yielding an error of less than about 1 dB.

§3. Results

To obtain the rich variety of dynamical behavior originating mainly from nonlinear instability, the possible transitions with $\varepsilon_{nl}=0$ and without Langevin noise in eqs. (1) and (2) are first studied. The output photon density exhibits multiple and submultiple spiking, a period doubling route to chaos, and hysteresis, whereas the self-pulsation phenomenon is not observed. Typical transition boundaries, in terms of driving frequency and modulation index, are depicted in Fig. 1 with dc bias current $I_b=1.5$. This figure provides us with a global view of possible transitions in the rate equations. The relevant features of the transitions are detailed in ref. 10. On the whole, the output photon density becomes spiky if the ac current is increased such that the minimum of the current swing approaches the threshold current level, i.e., $m\approx 0.5$. The output contains multiple spikes for $f < f_r$ and submultiple spikes for $f > f_r$, where f_r is the relaxation oscillation frequency and is approximately equal to 1.512 GHz in our case. The threshold PD_1 of period doubling with frequency variation from f_r to $2f_r$ shown in Fig. 1 possesses the minimum required ac current and is that which is most expected in the real experiment. In the following, the focus is on the PD_1 of the first onset of

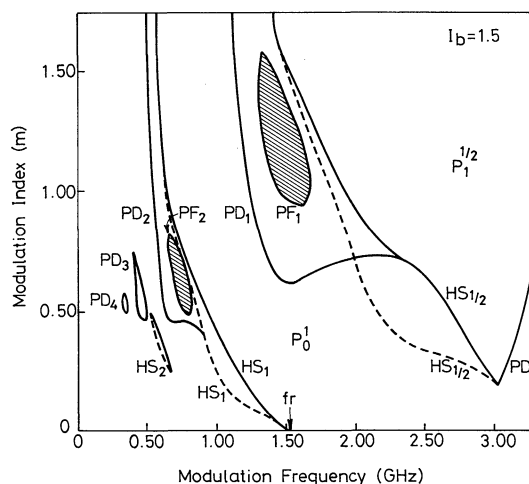


Fig. 1. Two-dimensional state diagram in terms of modulation index and modulation frequency at fixed dc bias $I_b=1.5$. P_n^m is the state of the photon density with m spikes and the n -th period doubling. Curve HS_m is the boundary of the hysteresis jump of photon density with m spikes; the section with the broken line denotes the downward jump. Curves PD_m and PF_m are the boundaries of period doubling and period-four of the photon density with m spikes, respectively.

period doubling.

Basically, the threshold of PD_1 is revealed as a U shape, as observed in the Toda oscillator,¹¹⁾ which possesses a potential well with exponential form in its dynamical equation. The phenomenon of bistability is also observed with the threshold curve $HS_{1/2}$ near PD_1 and has some influence on the occurrence of period doubling. Here, two kinds of period doubling can be observed. Both of them contain half-subharmonic components in the frequency domain and cannot be differentiated solely from the spectra. One is the normal type of period doubling and is unrelated to the hysteresis. The height of the two adjacent spikes of the output waveform is different, as shown in Fig. 2(a), and is denoted as type-I. It can be found using parameters away from the overlap section of curve $HS_{1/2}$. The other reveals only one spike within two periods, as in Fig. 2(b), and is denoted as type-II. Type-II period doubling often occurs accompanying hysteresis and can be found using the parameters on the overlap section of curves PD_1 and $HS_{1/2}$ in Fig. 1.

The dependence of the U-shaped PD_1 on increasing ε factor and with consideration of the noise effect are now examined. As illustrated in Fig. 3, curve (a) for $\varepsilon=0$ is lifted upward to curve (b) (without noise) or (c) (with noise) for $\varepsilon=0.01$. Also, the phenomenon of bistability disappears, only type-I PD can be found for a large ε factor. It implies that the onset point of PD is increased for the large ε case. In other words, the factor ε_{nl} contributes to the damping ratio and results in suppression of PD and other dynamical instability, whereas, the threshold of PD is reduced to a fractional part, as shown in curve 3(c) when the noise effect is taken into account. the details are described as follows.

To extract the influence of noise, first of all, we examine the spectrum of photon density without ac modula-

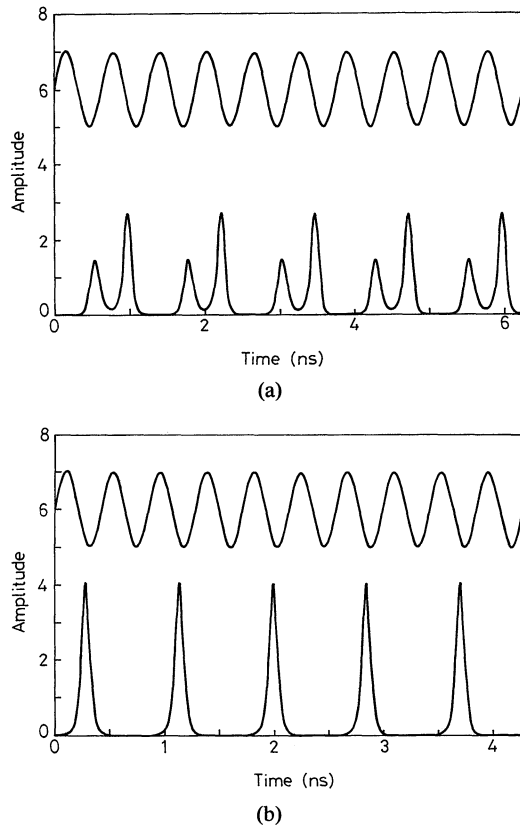


Fig. 2. (a) Time evolution with $f=1.6$ GHz and $m=0.85$ in P_1^1 ; (b) time evolution with $f=2.34$ GHz and $m=0.75$ in $P_1^{1/2}$.

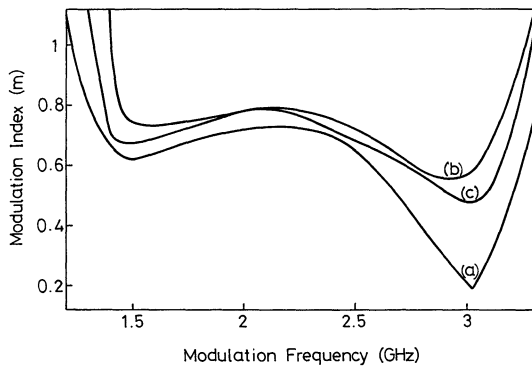


Fig. 3. U-shaped state diagram with (a) $\varepsilon=0.0$, (b) $\varepsilon=0.01$, and (c) $\varepsilon=0.01$ and Langevin noise.

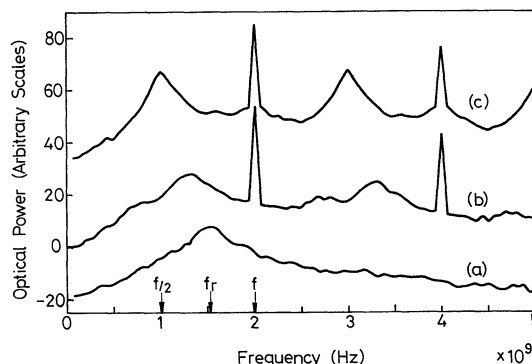


Fig. 4. The Fourier spectra at $f=2$ GHz, $I_b=1.5$, and (a) $m=0$, (b) $m=0.5$, and (c) $m=0.75$.

tion. It is characterized by intrinsic fluctuation with peak frequency centered around the relaxation oscillation frequency f_r , as shown in curve (a) of Fig. 4. The fluctuation level increases in amplitude and its peak frequency is gradually pulled toward $f/2$, i.e., the half-subharmonic of the modulation frequency, as the modulation index increases to a certain level, such as $m=0.5$ and 0.75 in curves (b) and (c) of Figs. 4, respectively. The peak near $f/2$ will enhance the emergence of PD. As seen in curves (b) and (c) of Fig. 3, the threshold for PD with noise involved is indeed reduced. The most significant reduction at about 10% occurs at $f \cong 2f_r$. According to our observation, when the external frequency is set to near, and less than, two times the relaxation oscillation, the noise spectra can be pulled toward $f/2$ to enhance the onset of period doubling. However, the effect of frequency pulling ceases when the corresponding subharmonic is too far away from the relaxation frequency f_r , and no obvious change in the threshold values can be found.

Next, the origin of the pulling phenomenon is further explored. It is evinced that two effects contribute to this phenomenon. One is that the laser diode pumped by a large ac signal with frequency f can be taken as a small-signal amplifier with maximum frequency response around $f/2$. Due to the nonlinear nature, the gain factor becomes increasingly significant with the peak closer to $f/2$ as the pumping approaches the onset of period doubling. This is one of the universal features of forced nonlinear oscillators.¹²⁾ The other is that, under small-signal operation, the laser diode described by the rate equations behaves like a parallel underdamped oscillator with maximum frequency response around the relaxation-oscillation frequency f_r . The relaxation bump shifts downward as the modulation index is increased. In view of these two effects, the ac-pumped laser diode has two peaks in its frequency response, as shown in Fig. 5. Accordingly, the broad-band Langevin noise input to the pumped laser diode is filtered and amplified to exhibit two bumps in accordance with these two peaks. When the relaxation peak coincides with the subharmonic gain peak, the amplification becomes prominent such that the occurrence of period doubling is significantly enhanced. In other words, the phenomenon of period doubling occurs more easily with less external driving as the driving frequency nears twice the relaxation frequency.

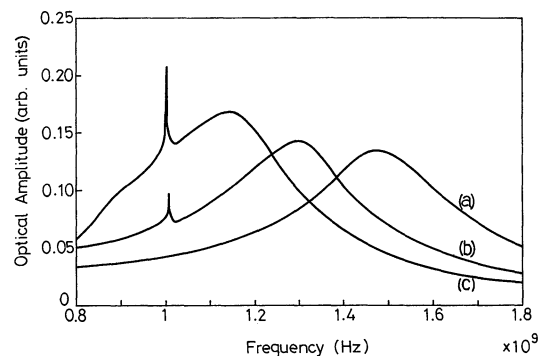


Fig. 5. The frequency responses of the ac-pumped laser diode with $I_b=1.5$ and (a) $m=0$, (b) $m=0.5$, and (c) $m=0.75$.

§4. Conclusions

In this letter we presented the various transitions of rate equations with applications to a semiconductor laser. The bistability and period doubling route occur repeatedly among the resonant regions in the lightly damped situation. The most profound event of period doubling with the U-shaped threshold is found in the frequency interval between f_r and $2f_r$. It is concluded that the noise bump near half the driving frequency is an important precursor of period doubling. We anticipate that all the relevant results of our work will provide a key for quantitative reference to most practical applications in actual experiments.

Acknowledgement

This study was supported by the National Science Council, Republic of China, under contract number: NSC79-0208-M009-28.

References

- 1) C. H. Lee, T. H. Yoon and S. Y. Shin: Appl. Phys. Lett. **46** (1985) 95.
- 2) Y. C. Chen, H. G. Winful and J. M. Liu: Appl. Phys. Lett. **47** (1985) 208.
- 3) M. Tang and S. Wang: Appl. Phys. Lett. **48** (1986) 900.
- 4) M. Tang and S. Wang: Appl. Phys. Lett. **50** (1987) 1861.
- 5) G. P. Agrawal: Appl. Phys. Lett. **49** (1986) 1013.
- 6) Y. Hori, H. Serizawa and H. Sato: J. Opt. Soc. Am. B **5** (1988) 1089.
- 7) L. Chusseau, E. Hemery and J. Lourtioz: Appl. Phys. Lett. **55** (1989) 822.
- 8) J. Katz, S. Margalit, C. Harder, D. Wilt and A. Yariv: IEEE QE-**17** (1981) 4.
- 9) D. Marcuse: IEEE J. Quantum Electron. QE-**20** (1984) 1139.
- 10) Y. H. Kao, C. H. Tsai and C. S. Wang: Rev. Sci. Instrum. **63** (1992) 75.
- 11) T. Klinker, W. Meyer-Ilse and W. Lauterborn: Phys. Lett. A **101** (1984) 379.
- 12) K. Wiesenfeld and B. McNamara: Phys. Rev. Lett. **55** (1985) 13.